applied sciences

MDPI

Article

Inundation Risk Assessment of Underground Space Using Consequence-Probability Matrix

Yong-sik Han, Eun Taek Shin, Tae Soo Eum and Chang Geun Song *

Department of Safety Engineering, Incheon National University, Incheon 22012, Korea; dydtlr11456@icloud.com (Y.-s.H.); euntaek.shin@outlook.com (E.T.S.); djaxotn00@inu.ac.kr (T.S.E.)
* Correspondence: baybreeze119@inu.ac.kr; Tel.: +82-32-835-8291

Received: 15 February 2019; Accepted: 18 March 2019; Published: 21 March 2019

Abstract: Increases in the frequency and severity of extreme rainfall might cause catastrophic submergence of underground spaces. Therefore, it is essential to predict the flood risk for proactive design. This study presents the methodology of acquiring risk level considering both flood intensity and evacuation difficulty. The flood momentum was computed by a 2D hydraulic flow model, and the flood intensity (FI) was employed to evaluate the consequence of flooding. To investigate the level of evacuation difficulty, the spatial layout of rooms, together with walking speed, were considered in the risk analysis process. If stormwater runoff enters an underground space, zones far away from the inlet usually have low risk levels. However, when the level of evacuation difficulty was considered, the risk level was dependent on the evacuation distance and location of the inlet and exit. If people are in zones with a risk level of 4 or 5, a rapid evacuation is necessary for preventing human casualties. The proposed methodology incorporated with the inundation model can be applied to any underground space regardless of the location of stairs, the number of exits, shape of rooms, or layout of the floor. Consequently, it will contribute to mitigating flood damage in an underground space.

Keywords: underground space; inundation; hydrodynamic modeling; evacuation difficulty; consequence –probability matrix

1. Introduction

With increasingly fast-paced industrialization, sudden climate change has been underway across the globe. This leads to an increase in the intensity and the frequency of heavy rainfall. In addition to continuing industrialization, urbanization is also proceeding at an unprecedented rate, with increases in the number and heights of buildings that are used for various purposes, such as residential, commercial, and public buildings. As the number of buildings in urban centers are reaching saturation, underground space is being increasingly utilized for underground facilities, such as subways, shopping malls, substations, parking lots, and many others, which are densely distributed underneath the urban area. As such complex facilities increase, covering more and more ground, impervious surfaces also continue to increase. Typically, the size of the impervious layer in Seoul was 7.8% in 1962, but rose to 47.7% in 2010 [1]. With the simultaneous progress of urbanization and climate change, the frequency of flood damage has also increased. The stormwater that accumulates on the ground moves to underground spaces along the roads drawn by the force of gravity and infiltrates the ground space through various pathways. The stormwater runoff that flows into underground spaces can cause human casualties and damage to property owing to its high flow velocity, despite its low water depth, as it rapidly gains in water pressure and momentum. Underground spaces vulnerable to flooding are becoming more complex and larger. Underground linked complex facilities have blind spots where safety cannot be secured and can therefore be very vulnerable to disasters, as presented in Figure 1.

Figure 1. Vulnerability of underground space.

Floods in an underground space are most likely to reach the lowest floor along the interlayer connection structure under the influence of gravity [2–4]. Moreover, various facilities and equipment installed in underground spaces, such as substations and utility pumps, can cause hybrid disasters through electric shock, power outage, fire, water service interruption, destroyed facilities, collapsed structures, and subsidence. In this context, higher priority must be made to safety as the number of underground facilities increase. Previous researches on urban inundation have normally been performed at the watershed scale and have typically involved flooding analysis of the targeted region, sewer network analysis, and impact evaluation of flood prevention measures. But there is a shortage of hydrodynamic-based modeling that analyzes, in detail, the flow submerging underground spaces [5].

Nowadays, a variety of models and approaches are used to determine inundation and flood damage [6–9]. However, there is a lack of hydrodynamic-based modeling that analyzes, in detail, the flow through underground access stairways. A numerical model is a favorable tool to predict the damage and range of flooding. Although a three-dimensional (3D) hydraulic model yields the most accurate analysis results for numerical simulations of flooding conditions, it is still time-consuming, and the analysis involves complicated processes owing to the excessive computational load due to the huge number of calculation grids. Therefore, it is desirable to apply a horizontal two-dimensional (2D) hydraulic model to calculate the flow velocity and flood depth in a flow field in both longitudinal (i.e., streamwise spreading) and transverse directions [10–12]. In some of the existing underground flood damage analysis studies, only the change of flood depth was analyzed according to the time of immersion in the underground space, and the type of damage was analyzed according to the flood damage history statistics of the underground flood.

In this study, to quantify the severity and the impact of flooding in an underground space, the concept of a consequence-probability matrix was used. The flood depth and the flow momentum were computed by a 2D hydraulic flow model, and the flood intensity (FI) was employed to evaluate the severity or the consequence of flooding [13]. In addition, to investigate the level of evacuation difficulty, the spatial layout of rooms and exit locations, together with walking speed, were considered in the risk analysis process.

2. Instability Due to Kinetic Energy of Stormwater during Flooding

Before analyzing flood risk in the underground space, the severity caused by storm flow force in order to estimate the degree of hydraulic force to the storm coming down with high velocity and high pressure through the inlet is described. Jonkman and Kelman confirmed that 25% of flood deaths in the Netherlands occurred while walking [14]. The two hydrodynamic mechanisms that can cause instability when humans encounter fast flow rates are distinguished by movement instability (toppling) and friction instability (sliding). Toppling occurs when the movement that tries to overturn the body is greater than the movement of body resistance. Sliding occurs when the force generated by the flow is greater than the friction resistance exerted between the human foot and surface. Foster and Cox conducted an experiment on instability in children in indoor experimental channels [15]. Physical conditions, mobility, and hydrodynamic flow influenced human stability. In the above experiment,

it was confirmed that sliding occurred because it was carried out under the conditions of low water level and high flow rate. Abt et al. suggested that instability for toppling was related to the water level [16]. However, the approximate function of this experience does not correlate the risk level with the physical effect. Jonkman and Rowsell extended the experimental data by conducting experiments under real conditions at low water levels and flow rates [17]. However, buoyancy was neglected in this experiment. Xia et al. performed a 1:5.5 geometric topology on human models [18]. In this experiment, they introduced the concept of buoyancy and developed a variable system for toppling and slipping failure mechanisms. They derived two formulas for critical velocity for slipping and toppling instability mechanisms, and conceptual models were introduced to explain human stability as a function of depth and flow rate to provide a framework for interpreting experimental activities. Love modeled the body as a rectangle and reflected the role of buoyancy in the instability that causes toppling [19]. Lind et al. corrected the relationship based on the product of flow velocity and depth, and derived conceptual and experimental formulas [20]. They proposed an equation for instability that models the human body as a solid circular cylinder and calculated the product of the critical depth and the velocity as a function of drag coefficient and immersion, resulting in toppling. Based on these experiments, the product of the flow velocity and the depth of water is the flow capacity in order to estimate human damage due to rainfall. Based on the above descriptions, this study also employed the product of the flow velocity and the depth as a flood intensity that determines the consequence of inundation.

3. Methods

In the previous study [5], the inundation analysis model was validated against an urban flooding problem. Targeting on the identical application site used in this study, the inundation results (flow depth and velocity) were intensively analyzed and parameter calibrations, including roughness coefficient and turbulent eddy viscosity, were mentioned. Following-up research of [5], this study presented the methodology of acquiring risk level considering both flood intensity and evacuation difficulty.

3.1. Model Descriptions

The governing equations of the two-dimensional flood analysis model for computing the hydrodynamic process of underground inundation stem from the conservation principles of mass and momentum [5].

$$\frac{\partial h}{\partial t} + h\nabla\cdot\underline{u} + \underline{u}\cdot(\nabla h) = Eh\sqrt{\underline{u}\cdot\underline{u}} \tag{1}$$

$$\frac{\partial \underline{u}}{\partial t} + (\underline{u}\cdot\nabla)\underline{u} = -g\nabla(H+h) + \frac{1}{h}\nabla\cdot(h\nu\nabla\underline{u}) - gn^2\frac{\sqrt{\underline{u}\cdot\underline{u}}}{h^{4/3}}\underline{u} - E(\underline{u}\cdot\underline{u}) \tag{2}$$

where t is the time, h is the inundation depth; $\underline{u} = (u, v)$ are the vertically averaged velocity vectors in the x- and y-directions, respectively; E is the transfer coefficient adjusting the magnitude of the flow moving to downstairs; H is a bottom elevation measured from datum; ν is the kinematic eddy viscosity; and n is the roughness coefficient.

The numerical approximation of the flow equations was implemented by the streamline diffusion finite element method [21,22]. The developed numerical model has a number of distinct features [23,24] and outperforms others in terms of stability and accuracy [25,26].

3.2. Risk Calculation

Prior to proceeding to the flood risk calculation, we proposed the risk calculation method commonly used in the field of safety engineering. As graphically displayed in Figure 2, the risk level was calculated from a combination of the probability of evacuation difficulty occurring in the horizontal axis, and the consequence of the flowing water materializing in the vertical axis. The detailed descriptions of risk calculation and matrix constitution are given as follows.

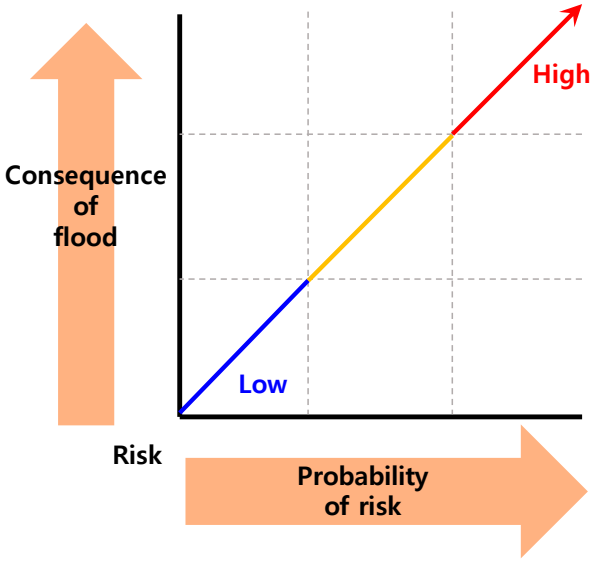

Figure 2. Risk calculation.

3.2.1. Constitution of Flooding Consequence

The flow impact of a flood at the time point for peak flow momentum was defined as "consequences" in the vertical axis (Figure 2). The consequences can also be obtained by calculating the relative risk with the product of the water depth and flow velocity of each of the nodes constituting the computational domain. This method of calculating the relative risk has the advantage of considering the locations of the inlets and exits and the relative spatial distribution of fluid forces, but it cannot estimate the consequences likely to be incurred by hydrodynamic fluid forces. Therefore, we introduced the concept of flood intensity (FI) [13]. FI was calculated as follows: If the flow velocity (v) at each node was lower than 1 m/s, FI was equal to the flood depth (h), and if the flow velocity (v) was 1 m/s or higher, FI was equal to the momentum (hv). The damage level based on the FI is presented in Figure 3. The FI was originally proposed by [13] to assess the flood hazard. Because FI can accurately provide hazard categories considering hydraulic impact exerted per unit area and density of water (hv) with less effort, it has been frequently used to predict the flood risk at the local spatial scale [11,27]. We calculated the risk level of each of the nodes based on the FI and arranged the nodes in ascending order of risk level, classifying the risk level in tertiles.

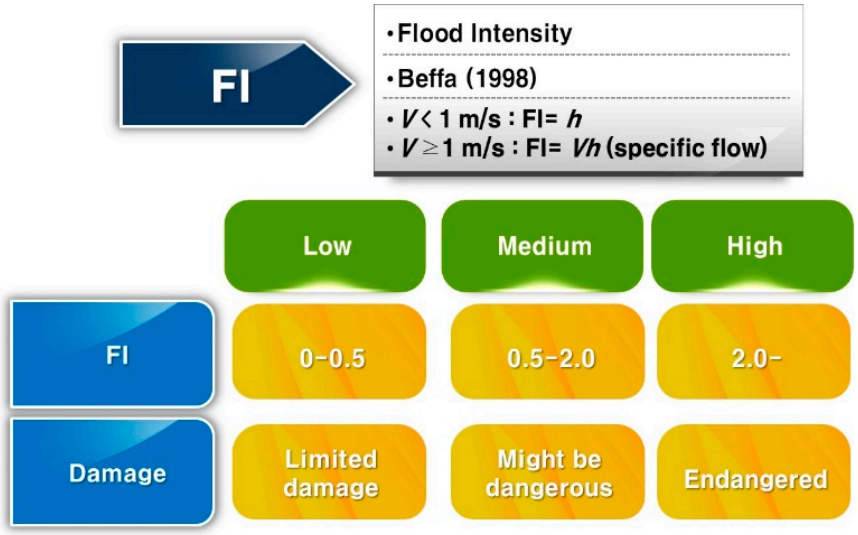

Figure 3. Flood intensity [13].

3.2.2. Constitution of Risk Probability

When applied to the flooding of an underground space, the probability became 1 in all cases because the stormwater continuously flowing into an underground space ended up spreading across the entire space within minutes or hours of exposure. In this case, it became difficult to define the horizontal axis. To overcome this problem, we introduced the concept of the level of evacuation difficulty in defining the risk probability. To estimate the level of evacuation difficulty, we partitioned the domain into zones according to their spatial layouts relative to the locations of the two stormwater inflow routes and two exits, as shown in Figure 4. Two exits were set at both ends, and the one at the shorter distance from the midpoint of each zone was set as the exit of the corresponding zone. The evacuation distance from each zone to the exit was calculated by adding the forward linear distances from the midpoint of each zone to the exit. As presented in Table 1, the walking speed was set at 0.7 m/s when the inflow depth was 0.4 m or lower, and 0.3 m/s when the inflow depth was 0.6 m or higher in accordance with the standards laid down by the Japan Building Disaster Prevention Association.

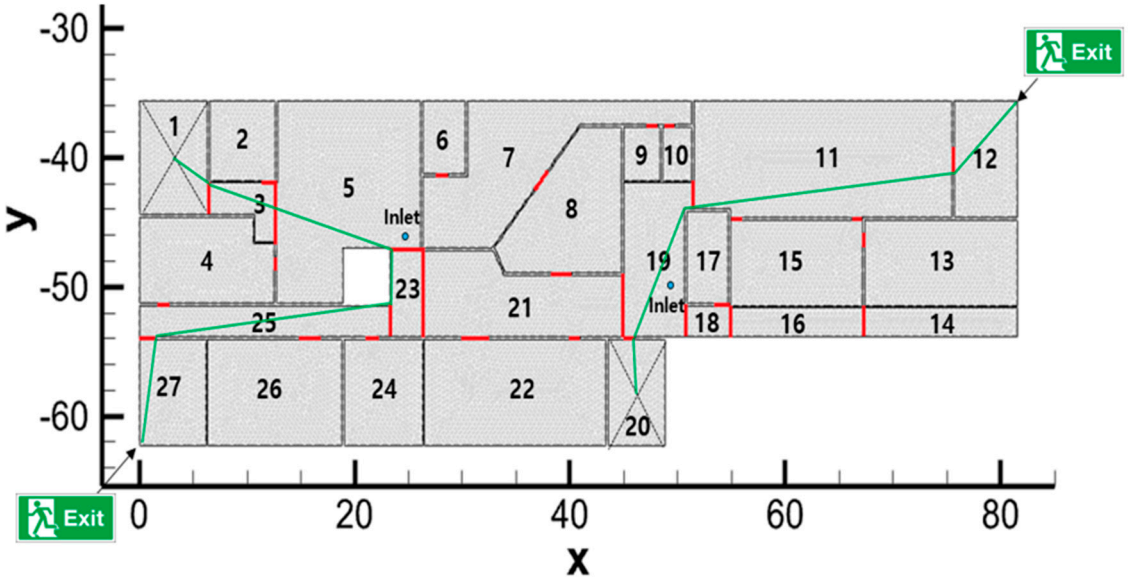

Figure 4. Space division to estimate difficulty of evacuation.

Table 1. Walking speed according to inflow depth.

Inflow Depth $\leq$ 0.4 m, Walking Speed = 0.7 m/s
Inflow Depth $\geq$ 0.6 m, Walking Speed = 0.3 m/s

As the input inflow depth was set at 1.0 m, the evacuation speed was set at 0.3 m/s. The evacuation time was calculated from the evacuation distance and walking speed. Table 2 lists the 27 zones (rooms) along with their respective exits, evacuation distances, and levels of evacuation difficulty in tertiles, with the third tertile being the highest level of evacuation difficulty.

Table 2. Exit selection and difficulty of evacuation.

Room Number	Respective Exit	Evacuation Distance	Difficulty of Evacuation	Room Number	Respective Exit	Evacuation Distance	Difficulty of Evacuation
1	A	57 m	3	15	B	24 m	1
2	A	52 m	3	16	B	50 m	3
3	A	49 m	2	17	B	48 m	2
4	A	17 m	1	18	B	42 m	2
5	A	42 m	2	19	B	37 m	2
6	A	64 m	3	20	B	48 m	2
7	A	57 m	3	21	A	43 m	2
8	B	50 m	3	22	A	45 m	2
9	B	68 m	3	23	A	33 m	1
10	B	69 m	3	24	A	33 m	2
11	B	10 m	1	25	A	21 m	1
12	B	5 m	1	26	A	27 m	1
13	B	27 m	1	27	A	5 m	1
14	B	64 m	3				

3.2.3. Flood Risk Matrix

Then, we calculated the flood risk after assigning the final FI across the domain using the flood risk matrix (Figure 5) by applying the level of evacuation difficulty and FI.

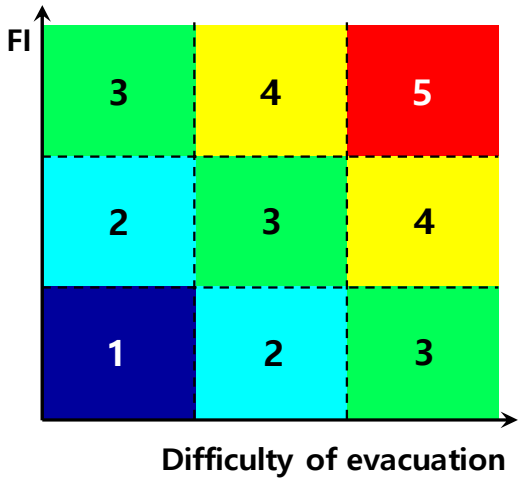

Figure 5. Flood risk calculation matrix.

4. Results

4.1. Application Site

The study area selected was the main building of the Korea Institute of Civil Engineering and Building Technology, located in Ilsan, Gyeonggi-do, Republic of Korea. The reasons why this site was chosen are as follows: The size of this office is moderate, its underground space has a number of separated rooms, and therefore the building can adequately represent a mid-sized underground space connected with the ground floor. The target application space has two stairs connected to the ground floor through which rainfall runoff can enter, as shown in Figure 6. We set two exits at both ends of the underground space.

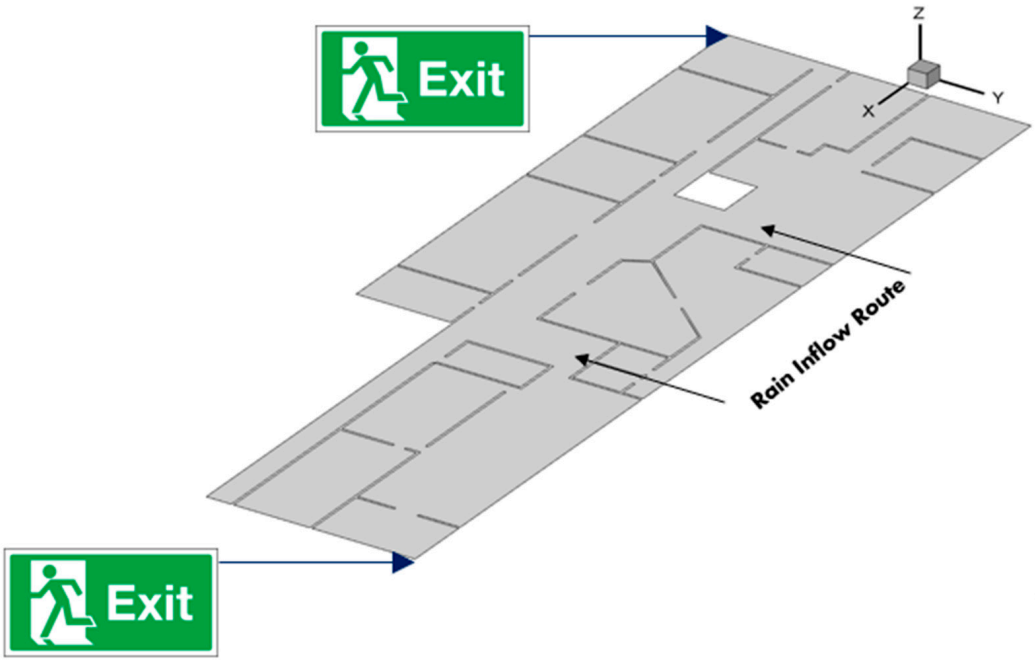

Figure 6. Application domain

4.2. Simulation Conditions

The flood risk level was computed based on the results of numerical simulations of the spatiotemporal flow characteristics (2D flow velocity and water depth) of the stormwater runoff flowing down through the two inflow routes. This section outlines the conditions and key assumptions for risk analysis.

According to [5], the velocity magnitude of the application site ranged from 0.0 to 1.8 m/s when water having a flow depth of 1.0 m kept entering from the main entrance of the ground floor. With these velocity values and subsequent inundation depth formation, the flow intensity may vary from low to medium to high. Therefore, the input depth of the stormwater entering the inlet was set at 1.0 m for flood risk calculations. If an inflow water depth higher than 1.0 m was assigned, the risk level would be increased all over the space. To achieve higher calculation accuracy, we partitioned the space into 27 zones according to their layouts. The shortest distance from the midpoint of each zone to each of the two exits was calculated, and the shorter route was determined as the evacuation route to the corresponding exit, as shown in Figure 7 (the green dotted line). The level of evacuation difficulty was then estimated based on the evacuation time considering walking speed.

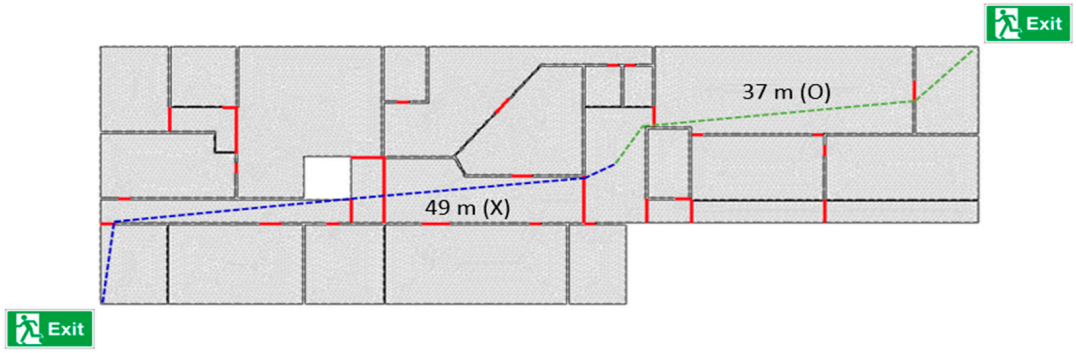

Figure 7. Exit selection.

4.3. Determination of Peak Risk

The following analysis was performed to estimate the peak risk level, the moment at which the flood momentum peaks, based on a flooding simulation up to 360 s at an interval of 0.2 s. The water

depth and flow velocity developed while stormwater was flowing into the domain through the two stairs connected to the ground floor and spreading across the domain. Once the underground space was filled to a certain water level, however, the flood depth was maintained at a constant level, and the flow velocity approached zero by reaching the stagnation point of the flow. In this paper, the peak risk level was therefore defined as the moment at which the stormwater inflow was spreading spatiotemporally at the highest flow velocity and flood depth.

In order to determine the time of risk estimation, the product of the inundation depth and the flow velocity of the rainwater spreading at each node for 1800 cases in a total of 360 s at intervals of 0.2 s was calculated. Then the average momentum was calculated. The instance at which the largest value was determined based on the average momentum was considered to be the representative risk assessment time point. As presented in Table 3, 50 s was determined as the time point for calculating the peak risk level, the moment at which the spatial mean momentum peaked, and the peak risk level was then calculated at 50 s using the spatiotemporal flow characteristics (flow velocity and depth) of the stormwater. Finally, we estimated the flood risk based on the level of evacuation difficulty of each zone.

Table 3. Risk assessment conditions.

Inflow Depth	Risk Assessment Time Point	Average Flow Momentum
1.0 m	50 s	0.046422

5. Discussions

Using the methods described in the previous section, we analyzed the flood risk from an input flood depth of 1.0 m. As the time point for the peak risk was assumed to be the moment of the highest spatial mean momentum (hv) of the stormwater spreading spatiotemporally with flood depth and flow velocity, we classified the momentum in tertile range, and listed the resulting mean momentums in Table 4.

Table 4. Tertile average moment.

Inflow Depth	1/3 Tertile Average Moment	2/3 Tertile Average Moment	3/3 Tertile Average Moment
1.0 m	1.000	1.04692	1.34408

In general, the flood risk is high in zones near the inlet and far away from the exit. However, owing to the structural characteristics of the study domain which contained two inlets at the center part of the entire space and two exits, the zones directly adjacent to the inlets did not show extremely high-risk levels (see Figure 8). Zones close to the inlets showed grade 2–3 flood risk levels if located near the exits, (i.e., they had low levels of evacuation difficulty). Those with high levels of evacuation difficulty showed grade 4–5 flood risk levels. For example, in the section located in the range of $-55 \leq y \leq -51$ m, two zones with x coordinates of $0 \leq x \leq 22$ m and $55 \leq x \leq 80$ m showed different risk levels owing to significantly different levels of evacuation difficulty, although both zones were located close to their respective exits. This suggests that the flood risk is affected by both the momentum (hv) of stormwater runoff and the level of evacuation difficulty, and that a rapid evacuation is essential for preventing human casualties in case of evacuations from locations near an inlet or with a high level of evacuation difficulty.

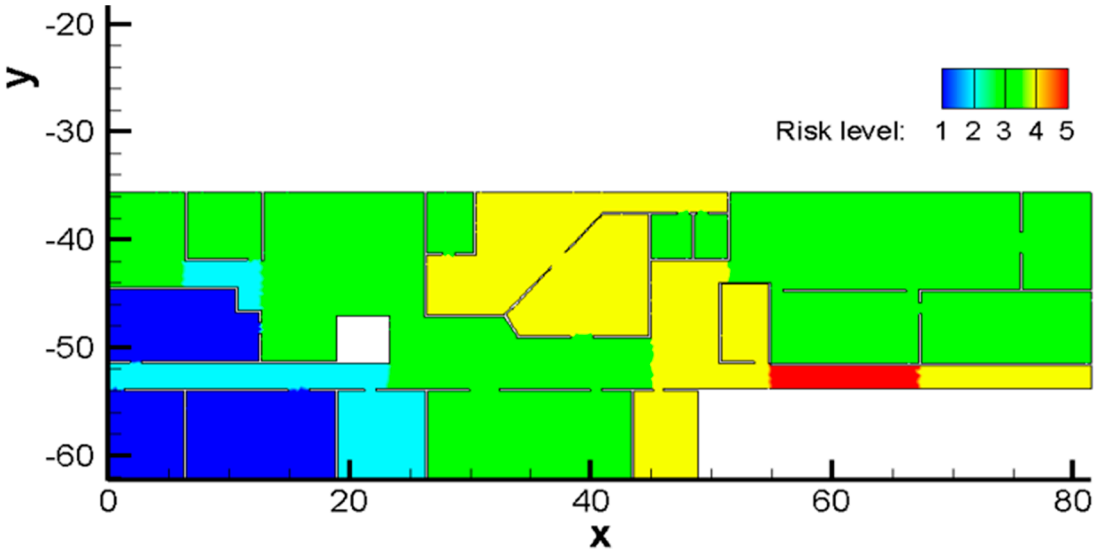

Figure 8. Inundation risk considering evacuation difficulty and hydrodynamic property.

6. Summary and Conclusions

Due to the urbanization and industrialization accompanied with climate change, the frequency and the intensity of heavy rainfall have been abruptly increasing, resulting in stormwater runoff flowing along the roads instead of being absorbed by pervious surfaces, causing underground spaces to flood. The stormwater flowing into underground spaces can lead to human casualties and cause damage to property owing to its high flow velocity, despite its low water depth, as it rapidly gains in water pressure and momentum. Accordingly, flood risk analysis is essential for enhancing the safety of underground spaces. However, previous research concerned with urban flooding has normally been conducted at the watershed scale and normally involved inundation analysis of the targeted region, sewer network analysis, and impact evaluation of flood prevention measures. The purpose of this study was to quantify flood risk by analyzing the flow momentum in the underground space connected to the ground floor. For quantitative analysis of underground space flood vulnerability, we calculated the flood risk, level of evacuation difficulty, and flood vulnerability index. For an accurate calculation of the risk level of the stormwater runoff entering an underground space through the stairs connected to the ground floor, it was necessary to calculate the inundation depth and its flow momentum associated with the flow velocity via hydrodynamic flow modeling. To do this, the flood depth and the momentum for the application site were obtained by a 2D hydraulic flow model, and the concept of flood intensity (FI) proposed by Beffa (1998) was employed to evaluate the severity or the consequence of flooding. In addition, to investigate the level of evacuation difficulty, the spatial layout of the rooms and exit location, together with walking speed, must be considered in the risk analysis process. In this concern, we partitioned the underground space into subzones according to the shape and layout of each room. Using the flood risk and level of evacuation difficulty thus calculated, we calculated the flood vulnerability index (FI) and assigned the FI grade to each subzone on a scale of 1 to 5.

If stormwater runoff enters an underground space at an input flood depth of 1.0 m, zones far away from the inlet usually have low risk levels, and the closer to the inlet, the higher the risk level. However, when the level of evacuation difficulty of the route from the zone concerned to the exit was considered, the FI 3 was estimated for the zones at longer distances from both the inlet and exit, and FI 3 for the zones at shorter distances from the inlet and longer distance from the exit. If people are in the zones with FI 4–5, a rapid evacuation is essential for preventing human casualties.

This study proposed a methodology to quantify the risk of underground flooding and can contribute to enhancing the accuracy of flood risk analysis and preventing human casualties and

damage to property by improving preparedness and disaster response measures in zones showing a high-risk level. Furthermore, the proposed methodology incorporated with the inundation model can be applied to any underground space regardless of the locations of the stairs, the number of exits, shape of rooms, or layout of the floor. Consequently, it will contribute to mitigating flood damage in underground spaces.

In a follow-up study, quantification of flood risk levels in various settings, such as different inlet configurations and large-scale building complexes with underground connections, will be explored. In addition, an automated algorithm for finding the optimal evacuation route based on the flood risk analysis is now being developed to furnish useful escape recommendation.

Author Contributions: Conceptualization, C.G.S.; formal analysis, Y.-s.H.; data curation, Y.-s.H., E.T.S. and T.S.E.; supervision, C.G.S.; writing—original draft, Y.-s.H.; writing—review and editing, C.G.S.

Funding: This research received no external funding.

Acknowledgments: This research was funded by a National Research Council of Science and Technology (NST) grant from the Korean government (MSIP) [No. CRC-16-02-KICT].

Conflicts of Interest: The authors declare no conflicts of interest.

References

1. Kapucu, N.; Liou, K.T. *Disaster and Development: Examining Global Issues and Cases*; Springer: Berlin/Heidelberg, Germany, 2014; p. 161.
2. Inoue, K. Study on its Application to Water Engineering and Numerical Analysis of Open Channel Unsteady Flow. Ph.D. Thesis, Kyoto University, Kyoto, Japan, 1986.
3. Ishigaki, T.; Toda, K.; Baba, Y.; Inoue, K.; Nakagawa, H. Experimental Study on Eevacuation from Underground Space by Using Real Size Models. *Proc. Hydraul. Eng. JSCE* **2006**, *50*, 583–588. [CrossRef]
4. Ko, D.W. Mitigation Effects on Urban Flood by Installing an Underground Storage Box. Ph.D. Thesis, Kyoto University, Kyoto, Japan, 2015.
5. Kim, H.J.; Rhee, D.S.; Song, C.G. Numerical Computation of Underground Inundation in Multiple Layers Using the Adaptive Transfer Method. *Water* **2018**, *10*, 85. [CrossRef]
6. Schubert, J.E.; Sanders, B.F. Building Treatments for Urban Flood Inundation Models and Implications for Predictive Skill and Modelling Efficiency. *Adv. Water Resour.* **2012**, *41*, 49–64. [CrossRef]
7. Zhang, T.; Feng, P.; Maksimovic, C.; Bates, P. Application of a Three-Dimensional Unstructured-Mesh Finite-Element Flooding Model and Comparison with Two-Dimensional Approaches. *Water Resour. Manag.* **2016**, *30*, 823–841. [CrossRef]
8. Ishigaki, T.; Kawanaka, R.; Ozaki, T.; Toda, K. Vulnerability to Underground Inundation and Evacuation in Densely Urbanized Area. *J. Disaster Res.* **2016**, *11*, 298–305. [CrossRef]
9. Bermudez, M.; Neal, J.C.; Bates, P.; Coxon, G.; Freer, J.; Cea, L.; Puertas, J. Quantifying Local Rainfall Dynamics and Uncertain Boundary Conditions into a Nested Regional-local Flood Modelling System. *Water Resour. Res.* **2017**, *53*, 2770–2785. [CrossRef]
10. Song, C.G.; Ku, T.G.; Kim, Y.D.; Park, Y.S. Floodplain stability index for sustainable waterfront development by spatial identification of erosion and deposition. *Sustainability* **2017**, *9*, 735. [CrossRef]
11. Song, C.G.; Ku, Y.H.; Kim, Y.D.; Park, Y.S. Stability analysis of riverfront facility on inundated floodplain based on flow characteristic. *J. Flood Risk Manag.* **2018**, *11*, S455–S467. [CrossRef]
12. Kim, S.E.; Lee, S.E.; Kim, D.W.; Song, C.G. Stormwater Inundation Analysis in Small and Medium Cities for the Climate Change Using EPA-SWMM and HDM-2D. *J. Coast. Res.* **2018**, *85*, 991–995. [CrossRef]
13. Beffa, C. Two-dimensional modelling of flood hazards in urban areas. In Proceedings of the 3rd International Conference on Hydroscience and Engineering, Berlin, Germany, 31 August–3 September 1998.
14. Jonkman, S.N.; Kelman, I. An Analysis of the Causes and Circumstances of Flood Disaster Deaths. *Disasters* **2005**, *29*, 75–97. [CrossRef] [PubMed]
15. Foster, D.N.; Cox, R. *Stability of Children on Roads Used as Floodways*; Tech. Rep. 13/73; UNSW Water Research Laboratory: Sidney, Australia, 1973.
16. Abt, S.R.; Wittler, R.J.; Taylor, A.; Love, D.J. Human Stability in a High Flood Hazard Zone1. *J. Am. Water Resour. Assoc.* **1989**, *25*, 881–890. [CrossRef]

17. Jonkman, S.N.; Rowsell, E.P. Human Instability in Flood Flows. *J. Am. Water Resour. Assoc.* **2008**, *44*, 1–11. [CrossRef]
18. Xia, J.; Falconer, R.A.; Wang, Y.; Xiao, X. New criterion for the stability of a human body in floodwaters. *J. Hydraul. Res.* **2014**, *52*, 93–104. [CrossRef]
19. Love, D.J. *Analysis of a High Hazard Flood Zone*; Technical Report prepared for City of Boulder Public Works Department; Love & Assoc. Inc.: Boulder, CO, USA, 1987.
20. Lind, N.; Hartford, D.; Assaf, H. Hydrodynamic models of Human Stability in a Flood. *J. Am. Water Resour. Assoc.* **2004**, *8*, 89–96. [CrossRef]
21. Song, C.G.; Oh, T. Transient SU/PG modelling of discontinuous wave propagation. *Prog. Comput. Fluid Dyn. Int. J.* **2016**, *16*, 146–162. [CrossRef]
22. Erath, C.; Praetorius, D. Optimal Adaptivity for the SUPG Finite Element Method. *arXiv*, **2018**; arXiv:1806.11000.
23. Lee, S.O.; Song, C.G. Influence of flow resistance stresses on debris flow runout. *Environ. Earth Sci.* **2018**, *77*, 426. [CrossRef]
24. Rhee, D.S.; Lyu, S.W.; Song, C.G. Numerical Computation of Rapid Flow over Steep Terrain Using Total Acceleration Method. *J. Coast. Res.* **2018**, *85*, 986–990. [CrossRef]
25. Song, C.G.; Seo, I.W.; Do Kim, Y. Analysis of secondary current effect in the modeling of shallow flow in open channels. *Adv. Water Resour.* **2012**, *41*, 29–48. [CrossRef]
26. Seo, I.W.; Song, C.G. Numerical simulation of laminar flow past a circular cylinder with slip conditions. *Int. J. Numer. Methods Fluids* **2012**, *68*, 1538–1560. [CrossRef]
27. Vojtek, M.; Vojteková, J. Flood hazard and flood risk assessment at the local spatial scale: A case study. Geomatics. *Nat. Hazards Risk* **2016**, *7*, 1973–1992. [CrossRef]